TESTING MODELS OF PEAK-RING IMPACT CRATER FORMATION. G. S. Collins[1], D. A. Kring[2] and R. W. K. Potter[3], [1]Department of Earth Science and Engineering, Imperial College, London, UK (g.collins@imperial.ac.uk), [2]Lunar and Planetary Institute, 3600 Bay Area Boulevard, Houston, TX, USA, 77058. [3]Department of Earth, Environmental and Planetary Sciences, Brown University, Providence, USA.

Introduction: A recent synthesis of morphometric, spectroscopic and gravity observations of lunar peak-ring impact craters [1] provides constraints for models of the formation of peak rings and the provenance of their constituent materials. Here we show that current numerical models of peak-ring crater formation are consistent with many of these observational constraints and explore the cause and implications of discrepancies.

Peak-ring basin observations: Recent spectral observations strongly support a crustal origin for peak rings on the Moon as nearly all peak rings exhibit extensive outcrops of pure anorthosite [1-5]. Moreover, areas of high-albedo, featureless spectra and boulder-rich outcrops in some peak rings have been proposed as locations of shocked plagioclase [5]. If correct, this observation implies that peak rings are comprised of rocks that have been exposed to a range of shock pressures up to and exceeding 25 GPa [5].

Combined profiles of LOLA-derived topography and GRAIL-derived crustal structure have also revealed a remarkable correlation between moho and surface structure [1]. All peak-ring basins show central mantle uplifts with diameters that correlate with the diameter of the peak ring. Outside this central mantle uplift is a collar of thickened crust, which is thickest near the midpoint between the peak-ring and rim crest and thins again to near the pre-impact crustal thickness around the position of the rim crest. It is unclear whether this correlation is coincidence or evidence that the crust-mantle boundary has a controlling influence on crater morphology.

Numerical modeling of peak-ring crater formation: Lunar peak-ring crater formation was simulated with the iSALE shock physics code [6]. We considered a range of crustal thicknesses from 20−60 km and assumed a vertical impact speed of 15 km/s, a surface gravity of 1.63 m/s^2 and a warm thermal gradient of 5 K/km in the upper 200 km. In all simulations, impactor and target mantle were modeled using a dunite material model; crust was modelled using a granite material model. ANEOS-derived equation of state tables were used to describe the thermodynamic state of both materials, while material strength was modeled using the approach described in [7]. To facilitate late stage crater collapse we used the block-oscillation model [8].

To examine the origin and shock state of peak ring materials, Lagrangian tracer particles that track the state of materials in the simulations were used to identify materials in the vicinity of the peak ring of the final simulated crater. To allow for possible disordering of peak-ring materials by small-scale faulting not resolved in our models, as suggested by observations of Schrödinger crater [9], and because it is difficult to define a precise location for the peak ring in the final simulated crater, we consider a relatively large volume as potential peak ring materials (70−90 km radius; <2 km depth below surface; Fig. 1B).

Provenance and shock state of peak ring materials: Model results show that peak ring materials originate from the crust at a range of depths and include a range of shock pressures (Fig. 1A). Volumetrically, peak ring materials are dominated by rocks that experienced peak pressures less than 25 GPa (Fig. 2A) and are derived almost entirely from the middle half of the crust (Fig. 2B). This is consistent with spectroscopic evidence for the provenance and shock state of peak ring materials [e.g., 5]. The peak ring materials originate along a streamtube (Fig. 1A) whose upper boundary is the streamline that divides the excavation zone—material ejected from the transient crater—and the displaced zone of the transient crater. Thus peak ring materials derive from depths comparable to (and shallower than) the maximum excavation depth [5].

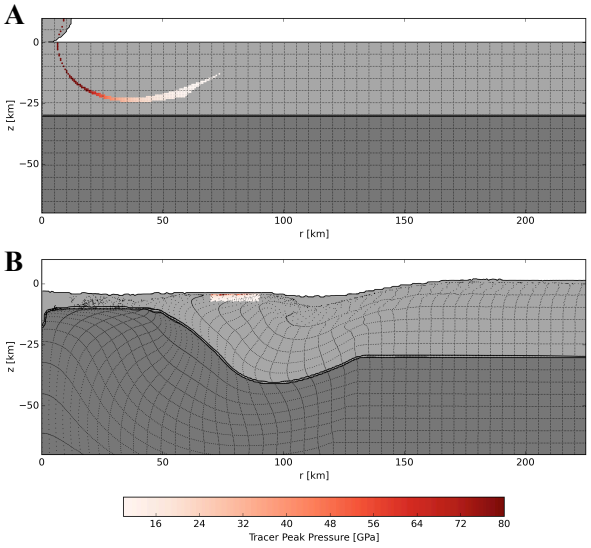

Figure 1. Provenance and peak shock pressure of peak-ring materials in a simulation of Schrödinger-scale impact crater formation (D_f ~ 350 km), assuming a 30-km thick crust. Peak ring materials originate from the crust at a range of depths just beneath the excavation cavity and comprise a range of shock pressures. Peak ring material is shown at its initial (A, top) and final (B, bottom) location.

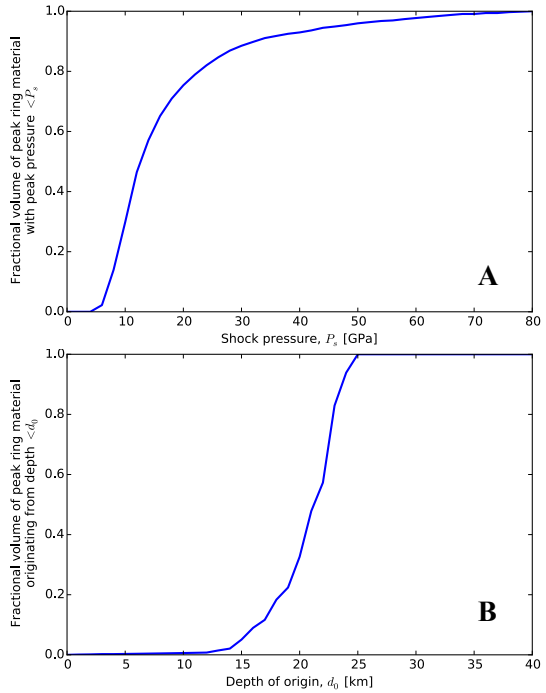

Figure 2. Distribution of peak shock pressure (top, A) and depth of origin (bottom, B) of peak ring materials for the model in Fig. 1. >80% of peak ring material experienced a peak shock pressure <25 GPa. Most peak ring material derives from mid-crustal depths (7.5−22.5 km).

Crater morphology and crustal structure: While the numerical simulations are able to reproduce observed final crater morphometry and qualitative crust-mantle structure quite well (Fig. 1), quantitative comparison of the crust-mantle structure reveals a subtle difference between the models and observation. In the Schrödinger-scale example shown in Fig. 1, the diameter of the mantle uplift is approximately the same as the peak-ring diameter; however, the annulus of thickened crust surrounding the mantle uplift is observed to be significantly thicker than GRAIL-derived crustal thickness profiles and its thickest point is just outside the peak ring, rather than midway between the rim crest and the peak ring as is observed. Reconciling these differences in the predicted topography of the crust-mantle interface should provide important clues for refining current numerical simulations and interpretations/models of gravity data over large impact basins on the Moon and other planetary bodies.

Kinematics of peak-ring formation: Two working hypotheses have evolved in the literature for peak-ring basin formation: one is based largely on numerical models [e.g., 10, 11] and the other, a conceptual geological model, is based largely on peak-ring observations, with facets similar to the model of [12] and the "nested melt-cavity model" [13]. Although these hypotheses have converged, a major outstanding question is whether peak-ring formation requires an over-heightened central peak. The kinematics of peak-ring formation in our numerical simulations is shown in Fig. 3. As the extent of overheightening of the central uplift drives the last phase of (outward) motion of the peak ring materials (D-E), it is possible that detailed structural mapping of peak rings [e.g., 9] may help differentiate between the two peak-ring formation hypotheses.

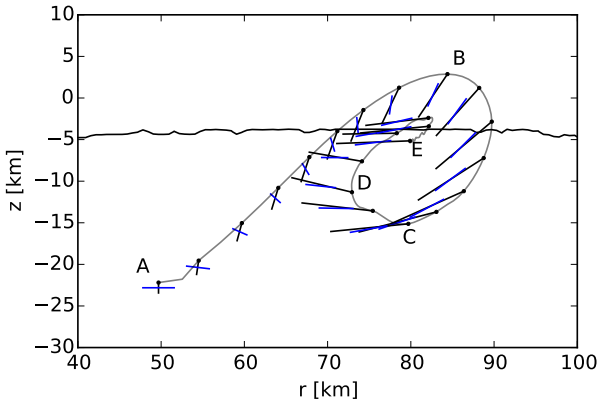

Figure 3. Kinematic depiction of representative motion of peak-ring material during crater formation for model in Fig. 1. Black and blue line segments connect two points within the peak ring material that are vertically and horizontally aligned at time zero, respectively (A). Peak-ring materials move upward and outward during excavation and undergo outward rotation. At the end of excavation they occupy a zone near the rim of the transient crater and horizontal layers are upturned (B). During crater modification (B-E) peak ring materials move inward and downward as the transient rim collapses (B-C) and then ride inward and upward as the central uplift overshoots the preimpact target (C-D). Further outward rotation occurs during this stage that inverts stratigraphy. The final movement of the peak-ring materials is outward and upward driven by the collapse of the central uplift (D-E).

Acknowledgements: We gratefully acknowledge NASA and STFC for funding and the developers of the iSALE shock physics code (www.isale-code.de). We thank DMH Baker and JW Head for stimulating discussion that prompted this work.

References: [1] Baker DMH, et al. (2016) *Icarus* doi: 10.1016/j.icarus.2015.11.033 [2] Ohtake M et al. (2009) *Nature* 461: 236–240. [3] Cheek LC et al. (2013) *JGR* 118: 1805–1820. [4] Kramer GY et al. (2013) *Icarus* 223: 131–148. [5] Baker DMH & Head JW (2015) *Icarus* 258: 164–180. [6] Wünnemann K et al. (2006) *Icarus* 180: 514–527. [7] Collins GS et al. (2004) *MAPS* 39: 217-231. [8] Wünnemann K and Ivanov BA (2003) *SSR* 51(13): 831–845. [9] Kring DA et al (2016) *47th LPSC* Abs. 1659. [10] Morgan JV et al. (2000) *EPSL* 183: 347–354. [11] Collins GS et al. (2002) *Icarus* 157: 24–33. [12] Cintala MJ & Grieve RAF (1998) *MAPS* 33: 889–912. [13] Head JW (2010) *GRL* 37(2): L02203.